Prospective Cell Sorting of Embryonic Rat Neural Stem Cells and Neuronal and Glial Progenitors Reveals Selective Effects of Basic Fibroblast Growth Factor and Epidermal Growth Factor on Self-Renewal and Differentiation

Dragan Maric, Irina Maric, Yoong Hee Chang, and Jeffery L. Barker
Laboratory of Neurophysiology, National Institute of Neurological Disorders and Stroke, National Institutes of Health, Bethesda, Maryland 20892

We directly isolated neural stem cells and lineage-restricted neuronal and glial progenitors from the embryonic rat telencephalon using a novel strategy of surface labeling and fluorescence-activated cell sorting. Neural stem cells, which did not express surface epitopes characteristic of differentiation or apoptosis, were sorted by negative selection. These cells predominantly expressed fibroblast growth factor receptor type 1 (FGFR-1), and a minority exhibited basic fibroblast growth factor (bFGF), whereas few expressed epidermal growth factor receptor (EGFR) or EGF. Clonal analyses revealed that these cells primarily self-renewed without differentiating in bFGF-containing medium, whereas few survived or expanded in EGF-containing medium. Culturing of neural stem cells in bFGF- and EGF-containing medium permitted both self-renewal and differentiation into neuronal, astroglial, and oligodendroglial phenotypes. In contrast, lineage-restricted progenitors were directly sorted by positive selection using a combination of surface epitopes identifying neuronal or glial phenotypes or both. These cells were also primarily FGFR-1$^+$, with few EGFR$^+$, and most expanded and progressed along their expected lineages in bFGF-containing medium but not in EGF-containing medium. Ca^{2+} imaging of self-renewing neural stem cells cultured in bFGF-containing medium revealed that bFGF, but not EGF, induced cytosolic Ca^{2+} ($Ca^{2+}{}_c$) responses in these cells, whereas in bFGF- and EGF-containing medium, both bFGF and EGF evoked $Ca^{2+}{}_c$ signals only in differentiating progeny of these cells. The results demonstrate that bFGF, but not EGF, sustains a calcium-dependent self-renewal of neural stem cells and early expansion of lineage-restricted progenitors, whereas together the two growth factors permit the initial commitment of neural stem cells into neuronal and glial phenotypes.

Key words: **fluorescence-activated cell sorting; negative selection; positive selection; neural stem cells; lineage-restricted progenitors; growth factors; calcium imaging**

Introduction

Self-renewing, multipotent neural stem cells have received increasing attention, both to study neuronal and glial cell lineage progression and to provide a possible therapeutic strategy for transplantation and regeneration of neural tissue (for review, see Cameron and McKay, 1998; Gage, 2000; Anderson, 2001; Temple, 2001). However, most *in vitro* studies of neural stem cells to date have involved retrospective analyses of heterogeneous populations of neuroepithelial or germinal zone cells, which were derived from the CNS and then cultured under selective growth conditions (Chu and Gage, 2001; Kornblum and Geschwind, 2001). Neural stem cells in these studies were inferred from the discovery of cells with the classic self-renewing and multipotential characteristics attributed to these cells. Recently, neural stem cells have been isolated directly from the embryonic peripheral nervous system (Morrison et al., 1999) and adult CNS (Rietze et al., 2001) using a positive selection strategy involving expression of surface epitopes in combination with fluorescence-activated cell sorting (FACS). These studies revealed the feasibility of using a FACS strategy to access neural stem cells for prospective analyses into the requirements for lineage progression.

In this regard, we have found previously that specific gangliosides and other epitopes appear on the cell surface of proliferating progenitors during the earliest phases of neuronal and glial lineage progressions throughout the embryonic rat CNS (Maric et al., 1999, 2000c). We reasoned that neural precursor cells, which do not yet express these epitopes, might be a source of neural stem cells. To test this hypothesis, we combined fluorescent labeling of five surface epitopes characteristic of differentiating or apoptotic cells with a negative selection FACS strategy to isolate a quintuple epitope-negative (QN) population of putative neural stem cells directly from embryonic rat telencephalon. With the same epitopes, a positive selection strategy was used to isolate lineage-restricted progenitor cells expressing specific patterns of surface gangliosides.

Sorted cells were then cultured in defined media supplemented with selected growth factors to investigate their lineage potential. Previous studies have revealed that basic fibroblast growth factor (bFGF) and fibroblast growth factor receptor 1 (FGFR-1) are expressed during neurogenesis (Weise et al., 1993; Baird, 1994). Furthermore, bFGF and epidermal growth factor

Received June 18, 2002; revised Oct. 17, 2002; accepted Oct. 22, 2002.

Correspondence should be addressed to Dragan Maric, Laboratory of Neurophysiology, National Institute of Neurological Disorders and Stroke, National Institutes of Health, Building 36, Room 4A-24, Bethesda, MD 20892. E-mail: maricd@ninds.nih.gov.

 0270-6474/02/220240-12$15.00/0

(EGF) have been used extensively to propagate neuroepithelial cells *in vitro* (for review, see Rao, 1999). In this study, we show that most telencephalic precursor and progenitor cells express FGFR-1, with a minority expressing bFGF and few expressing EGF or EGF receptor (EGFR). Negatively selected QN cells additionally express nestin, a characteristic marker of immature neuroepithelial cells (Hockfield and McKay, 1985), but are devoid of differentiating epitopes. In bFGF-containing medium, these cells primarily self-renewed, whereas in bFGF- and EGF-containing medium, these cells either self-renewed or differentiated into neuronal and glial phenotypes, thus revealing their multipotential capability and identifying them as neural stem cells. Positively selected progenitors primarily expanded and progressed along their expected lineages in bFGF-containing medium but not in EGF-containing medium. These results show that bFGF and EGF have differential effects on the self-renewal and early lineage progression of neural stem cells, which parallel the expression of growth factor regulation of Ca^{2+} levels.

Materials and Methods

Cell preparation

Experiments were performed on embryos recovered from timed pregnant Sprague Dawley rats (Taconic Farms, Germantown, NY). The embryonic (E) age was determined by comparing the crown–rump lengths of embryos with previously published values (Hebel and Stromberg, 1986). The research was performed in compliance with the Animal Welfare Act and the Public Health Service Policy on Humane Care and Use of Laboratory Animals and was approved by the National Institute of Neurological Disorders and Stroke Animal Care and Use Committee.

Telencephalic tissues from E13 embryos were used as a primary source of neural stem cells and early neuronal and glial progenitors for fluorescence-activated cell sorting and experimentation *in vitro* (see below). The tissues were optimally dissociated into single-cell suspensions, as described previously (Maric et al., 1997, 1998). During initial cell preparation, labeling of surface epitopes, and FACS sorting (see below), the cells were maintained in a normal physiological medium (NPM) supplemented with 1 mg/ml bovine serum albumin (BSA). The NPM itself consisted of (in mM): 145 NaCl, 5 KC1, 1.8 $CaCl_2$, 0.8 $MgCl_2$, 10 glucose, and 10 HEPES (all obtained from Sigma, St. Louis, MO), with pH and osmolarity adjusted to 7.3 and 290 mOsm, respectively.

Labeling of surface epitopes in single-cell suspensions

E13 telencephalic cells were surface-labeled using lineage-specific markers, as described previously (Maric et al., 1999, 2000c). Briefly, neuroglial and O-2A glial progenitors were immunoidentified using a mouse monoclonal class IgM anti-A2B5 (Roche Molecular Biochemicals, Indianapolis, IN) and JONES (Sigma) antibodies and visualized with phycoerythrin (PE)-conjugated goat anti-mouse IgM antibody (Caltag Laboratories, Burlingame, CA). Neuronal progenitors and differentiating neurons were revealed by binding of their surface gangliosides to biotinylated-cholera toxin B subunit (ChTx; Sigma) and a mixture of tetanus toxin fragment C (TnTx; Roche Molecular Biochemicals) and a mouse monoclonal class IgG2b anti-TnTx antibody (obtained from Dr. William Habig, Food and Drug Administration, Bethesda, MD). These primary reactions were visualized using PE- and carbocyanine dye (CY5)-conjugated streptavidin and PE/CY5-conjugated goat anti-mouse IgG2b antibody (Caltag), respectively. Differentiating oligodendroglial cells were directly stained with fluorescein isothiocyanate (FITC)-conjugated anti-O4 and anti-O1 antibodies (obtained from Dr. Rick I. Cohen, National Institute of Neurological Disorders and Stroke, National Institutes of Health), whereas the resident microglial cells were first immunoreacted with mouse monoclonal class IgG2a anti-CD11b antibody (clone OX-42; Serotec Inc., Raleigh, NC) and then visualized with PE-conjugated goat anti-mouse IgG2a antibody (Caltag). FITC-conjugated Annexin V (Trevigen Inc., Gaithersburg, MD) was used as an additional surface marker in conjunction with forward angle light scatter (FALS), a property related to cell size, to discriminate among apoptotic, necrotic, and nonapoptotic cells (see below and Fig. 1). All surface-labeling reactions were performed in NPM and BSA at 8°C.

Flow cytometric analysis and cell sorting

Surface-labeled telencephalic dissociates were analyzed, and different subpopulations were sort-purified using a FACSTAR$^+$ flow cytometer (Becton Dickinson, Mountain View, CA), according to previously published methods (Maric et al., 1999, 2000c). Briefly, the FITC, PE, and PE/CY5 fluorescence signals on individual cells were excited by an argon ion laser (model 2016; Spectra Physics, Mountain View, CA) tuned to obtain 500 mW power at 488 nm, and the resulting fluorescence emissions from each cell were collected using bandpass filters set at 530 ± 30, 575 ± 25, and 670 ± 20 nm, respectively. Cell Quest acquisition and analysis software (Becton Dickinson) was used to quantify the fluorescence signal intensities and FALS properties among the immunolabeled subpopulations and to set logical electronic gating parameters designed for sorting of neural precursors from differentiating progenitors using negative or positive selection strategies, respectively (see Fig. 1). The cells were physically sorted by deflecting electrically charged saline droplets containing single cells into appropriate test tubes. The viability of the sort-purified cells remained >96%, as confirmed by trypan blue exclusion.

bFGF, FGFR1, EGF, and EGFR immunolabeling

Telencephalic dissociates were surface-labeled and sorted into neural precursor and progenitor subpopulations, as shown in Figure 1. Aliquots of sorted cells were fixed in 4% paraformaldehyde (PF) and then washed in Dulbecco's PBS (Quality Biological, Inc., Gaithersburg, MD) supplemented with 1 mg/ml BSA and immunolabeled with rabbit anti-EGF antibody (Sigma) or rabbit anti-EGFR, anti-FGF-2, or anti-FGFR-1 antibodies (Santa Cruz Biotechnology, Santa Cruz, CA) for 1 hr at room temperature (RT). The primary immunoreactions were visualized after a 30 min incubation at RT with FITC-conjugated donkey anti-rabbit IgG secondary antibody (Jackson ImmunoResearch, West Grove, PA). The fluorescence signal intensities among the immunolabeled subpopulations were quantified by FACS, as described above.

Cell culture

Sort-purified neural precursor and progenitor cells were plated at clonal density (1×10^3 cells/cm^2) on poly-D-lysine-coated (Sigma) and bovine plasma fibronectin-coated (Invitrogen, Frederick, MD) coverslips, which were photo-etched with an alphanumeric grid (Bellco Glass Inc., Vineland, NJ) and preglued to 35 mm tissue culture dishes (MatTek Corp., Ashland, MA). The grid facilitated relocation of the same field of cells during multiepitope immunostaining protocols (see below). Individual cells were followed over a 7 d period using an Axiovert 135 inverted microscope (Zeiss, Thornwood, NY). The cells were cultured in Neurobasal Medium (Invitrogen) supplemented with 1× working stock of B27 additives (diluted 50-fold from commercially available stock; Invitrogen) and one of the following growth conditions: 10 ng/ml human recombinant bFGF (Intergen Co., Purchase, NY), 10 ng/ml human recombinant EGF (Sigma), or 10 ng/ml bFGF together with 10 ng/ml EGF. In some experiments with neural precursor cells, the initial concentrations of bFGF and EGF were increased to 100 ng/ml in the culture medium, whereas in others, the 10 ng/ml dose was replenished every 48 hr during the 7 d culture period. We also tested the effects of withdrawal of each growth factor after 24 hr and 5 d in culture on the proliferative and differentiating potential of these cells.

Labeling of surface, cytoplasmic, and nuclear epitopes in cell cultures

Surface epitope labeling. The protocol was generally identical to that used for dissociated cells in suspension (see above). The only exceptions were (1) direct labeling with FITC-conjugated ChTx (Sigma), thus allowing double staining with TnTx-anti-TnTx-PE/CY5; and (2) direct immunostaining with PE-conjugated anti-A2B5 (obtained from Dr. Rick I. Cohen), thus allowing double staining with FITC-conjugated O4 or O1.

Cytoplasmic epitope labeling. Cells in culture were also immunoidentified using lineage-specific cytoskeletal markers, as described previously (Maric et al., 2000c). These included mouse monoclonal class IgG1 anti-

nestin antibody (Department of Biological Sciences, University of Iowa, Iowa City, IA), which identifies neuroepithelium-derived precursor and progenitor cells (Hockfield and McKay, 1985), mouse monoclonal class IgG2a anti-tubulin β III antibody (TuJ1; Berkeley Antibody Co., Richmond, CA), which labels differentiating neurons, and rabbit polyclonal anti-glial fibrillary acidic protein antibody (GFAP), which identifies astrocytes (Chemicon International, Temecula, CA). Briefly, the cells were fixed in 4% PF and then washed in PBS and BSA and immunoreacted with anti-nestin, anti-TuJ1, and anti-GFAP antibodies. Nestin was visualized with biotinylated-goat anti-mouse IgG1 (Jackson ImmunoResearch), followed by aminomethylcoumarin (AMCA)-conjugated streptavidin (Jackson ImmunoResearch). TuJ1 and GFAP immunoreactions were visualized with PE-conjugated goat anti-mouse IgG2a (Caltag) and tetramethyl rhodamine isothiocyanate (TRITC)-conjugated goat anti-rabbit IgG (Southern Biotechnology Associates, Inc., Birmingham, AL) secondary antibodies, respectively.

Nuclear epitope labeling. Actively proliferating cells were identified using the thymidine analog 5-bromo 2′deoxyuridine (BrdU; Sigma), as described previously (Maric et al., 1997). Briefly, the protocol initially included a BrdU-labeling period either *in vivo* or *in vitro*. *In vivo* labeling involved a single intraperitoneal injection of 50 μg of BrdU/gm body weight into E13 dams, followed by killing 2 hr later. Otherwise, proliferating cells were cumulatively labeled *in vitro* with 10 μM BrdU for 2–24 hr before termination of culture. To detect incorporated BrdU, the cells were fixed in 70% ethanol (EtOH) at −20°C and then permeabilized, and their DNA was denatured with 2N HCl and 0.5% Triton X-100, and incorporated BrdU was visualized with FITC-conjugated mouse monoclonal class IgG1 anti-BrdU antibody (Becton Dickinson).

Multiepitope labeling protocols. Multiepitope staining protocols were applied to detect surface, cytoplasmic, and nuclear epitopes on repeatedly labeled fields of cells, using different combinations of subtype-specific, fluorochrome-conjugated primary or secondary antibodies or fluorochrome-conjugated ligands, followed by sequential photobleaching and restaining. Using an eight-epitope staining protocol, the cells were first pulse-labeled with BrdU and then directly surface-immunoreacted with fluorochrome-conjugated anti-O4-FITC and anti-A2B5-PE antibodies and subsequently imaged using an appropriate camera and optics mounted on an Axiovert 135 inverted fluorescence microscope (see below). After imaging, the remaining fluorescence signals were completely photobleached, and the cells were surface-relabeled with ChTx-FITC and TnTx-anti-TnTx-PE/CY5 and then fixed in 4% PF for 30 min at RT, washed in PBS and BSA, and relocated in the 35 mm culture dish using the underlying alphanumeric grid, and the resulting fluorescent signals were imaged and then photobleached, as described above. The cells were then fixed in 70% EtOH for 20 min at RT; their DNA was denatured in 2N HCl and 0.5% Triton X-100; and the cells were sequentially reimmunoreacted with anti-nestin-AMCA, anti-TuJ1-PE, anti-BrdU-FITC, and anti-GFAP-TRITC antibodies. The indirect immunostaining with anti-nestin-AMCA was followed by a blocking reaction with 50 μg/ml unlabeled mouse IgG (Sigma) for 30 min at RT before application of direct immunolabeling with anti-BrdU-FITC. Because there was spectral overlap between PE and TRITC, anti-GFAP-TRITC staining was preceded by anti-TuJ1-PE immunolabeling, which was completely photobleached after imaging. In another seven-epitope staining protocol, the cells were first surface-immunoreacted with anti-O4-FITC and anti-A2B5-PE and then imaged, photobleached, and restained with anti-O1-FITC and anti-OX42-PE. Subsequently, the cells were fixed in PF and then in EtOH and sequentially immunoreacted with anti-nestin-AMCA, anti-BrdU-FITC, and anti-GFAP-TRITC. In optimizing the multiepitope staining protocols, we have performed all the appropriate control experiments to confirm the specificity of each immunoreagent. Control immunoreactions using "simple" single-, double-, or triple-staining protocols revealed no significant cross-epitope immunoreactivity among primary or secondary antibodies.

Analysis of fluorescence signals. Phase-contrast and fluorescence signals were imaged using an Axiovert 135 inverted fluorescence microscope (Zeiss) equipped with an intensified charge-coupled device (ICCD) camera (Atto Instruments, Rockville, MD), as described previously (Maric et al., 2000b). The cells were illuminated with a 100 W mercury arc lamp (Zeiss), and the resulting fluorescence emissions were collected through a Fluar 40×, 1.3 oil phase 3 objective (Zeiss) using standard FITC-PE-PE/CY5 and FITC-TRITC-AMCA filter sets (Omega Optical, Brattleboro, VT). Fluorescence emissions for each fluorochrome signal were separately captured as eight-bit images, using the video sensor of the ICCD camera at 512 × 480 pixels resolution, and analyzed using Adobe Photoshop software (Adobe Systems, Inc., San Jose, CA).

Calcium imaging

Changes in cytosolic Ca^{2+} (Ca^{2+}_c) levels in response to bFGF and EGF were measured according to previously described methods (Maric et al., 2000a,b). Briefly, the cells were loaded with fura-2 AM and imaged at 1 sec intervals using the Attofluor RatioVision workstation (Atto Instruments). All recording solutions were warmed to 37°C and delivered to the 150 μl recording chamber using gravity-driven perfusion at a constant flow rate of ~2 ml/min. After imaging, the field of recorded cells was photographed using phase contrast optics and then washed in PBS and BSA and sequentially immunoidentified using the multiepitope staining protocols, as described above. In this way, the Ca^{2+}_c responses of individual cells to bFGF and EGF could be correlated precisely with their epitope expression patterns, which were used to identify their precursor, progenitor, or differentiated state.

Results

Fluorescence-activated cell sorting of neural precursors and progenitors

The multiepitope staining protocol for FACS sorting used only those surface epitopes that are already expressed in the rat telencephalon at E13 (Maric et al., 1999, 2000c) and that identify early neuronal, neuroglial, and oligodendroglial progenitors (Fig. 1*A1,A2*). There was no surface labeling with anti-O4, anti-O1, or anti-OX42 or cytoplasmic labeling with anti-GFAP immunoreactions (data not shown), which indicated that E13 telencephalic dissociates were devoid of well differentiated oligodendroglial, microglial, and astroglial populations. Approximately 60% of the cells in the E13 dissociate were labeled with ChTx, TnTx, A2B5, or JONES, whereas ~40% did not label with any of these markers (Fig. 1*A2*). We classified all ChTx- and TnTx-expressing cells ($ChTx^+TnTx^+A2B5^+JONES^+$ and $ChTx^+TnTx^+A2B5^-JONES^-$) as early neuronal progenitors or differentiating neurons (Fig. 1*A1,A2*; also refer to Table 2). Furthermore, we classified $ChTx^-TnTx^-A2B5^+JONES^+$ cells with low levels of A2B5 or JONES expression as putative bipotential neuroglial progenitors (Fig. 1*A1,A2*), which can differentiate into either neurons or oligodendroglia (refer to Table 3), and those with high levels of A2B5 or JONES labeling (Fig. 1*A1,A2*) as more restricted oligodendroglial progenitors (refer to Table 4). We hypothesized that the remaining unlabeled ($ChTx^-TnTx^-A2B5^-JONES^-$) precursor cells might be a source of putative neural stem cells (Figs. 1*A1,A2*, 2; Table 1).

To identify a vital population of neural stem cells, we additionally analyzed their FALS characteristics, a flow cytometric property that directly reflects cell size and integrity, in combination with Annexin V labeling, which identifies cells progressing through apoptosis (Koopman et al., 1994; Martin et al., 1995). Only vital cells exhibited high FALS values without detectable Annexin V staining (Fig. 1*B1,B2*). These cells did not significantly stain with trypan blue or propidium iodide after sorting (data not shown). Altogether, we used six parameters simultaneously (FALS and Annexin V, ChTx, TnTx, A2B5, and JONES labeling) to identify putative neural stem cells from the E13 telencephalon. Only those cells with high-FALS properties, not expressing the five surface epitopes ($ChTx^-TnTx^-A2B5^-JONES^-Annexin\ V^-$), hence quintuple epitope-negative (QN) cells, were considered vital neural stem cells and were sorted by negative selection for further study *in vitro*. The lack of these epitopes implied that these cells were not yet overtly

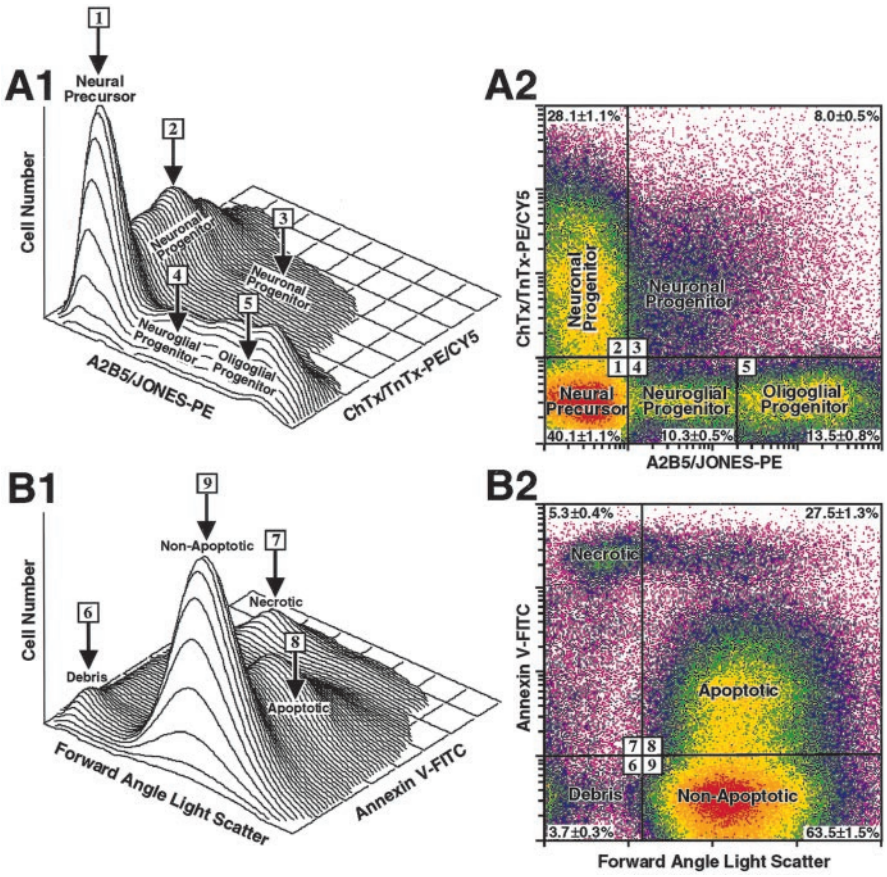

Figure 1. Surface epitope selection strategy to isolate neural precursor and progenitor cells using flow cytometry. *A1, A2*, Dissociates of E13 cortical neuroepithelial cells were simultaneously surface-labeled with ChTx-PE/CY5 in combination with TnTx-PE/CY5 to optimally resolve the neuronal progenitors and with A2B5-PE in combination with JONES-PE to optimally resolve neuroglial and early oligodendroglial progenitors. *B1, B2*, Annexin V–FITC binding was used as a fifth label together with FALS, a measure of particle size, to identify cell debris and necrotic, apoptotic, and nonapoptotic (vital) neural precursor and progenitor cells. Fluorescence and FALS signals were quantified on ~100,000 randomly sampled cells using the FACSTAR$^+$ flow cytometer (see Materials and Methods) and analyzed as three-dimensional contour plots (*A1, B1*) and corresponding two-dimensional log–log dot density plots (*A2, B2*). Boundaries in *A2* have been drawn empirically to delineate and quantify the unlabeled neural precursor cells (region *1*) and selectively labeled neuronal (regions *2, 3*), neuroglial (region *4*), and oligoglial progenitor (region *5*) subpopulations and in *B2* to delineate cell debris (region *6*), necrotic cells (region *7*), apoptotic cells (region *8*), and nonapoptotic cells (region *9*). The percentages of cells (mean ± SEM) in each subpopulation from 40 independent experiments are shown as *insets* in their respective delineated regions. A vital subpopulation of neural precursor cells lacking all five of the surface epitopes (i.e., ChTx$^-$TnTx$^-$A2B5$^-$JONES$^-$Annexin V$^-$) was sorted by negative selection, which involved the inclusion of cells in regions *1* and *9* and exclusion of cells in regions *2–8*. Viable, nonapoptotic subpopulations of neuronal, neuroglial, or oligoglial progenitors were sorted using a positive selection strategy, which involved the inclusion of cells delineated in regions *2–5* and the exclusions of cell debris in region *6* and cells with necrotic and apoptotic attributes in regions *7* and *8*.

committed either to differentiate or to die. Because 40.1 ± 1.1% (mean ± SEM) of the cells from E13 dissociates were ChTx$^-$TnTx$^-$A2B5$^-$JONES$^-$ (Fig. 1*A2*), and 46.1 ± 1.6% of these were Annexin V$^+$ (data not shown), the total starting population of viable QN cells before sorting averaged ~22% of all E13 telencephalic cells. Furthermore, by combining the above vital cell criteria with selected patterns of surface epitope expression characteristic of differentiating cells, a positive selection strategy was used to sort neuronal, neuroglial, and oligoglial progenitors (Fig. 1).

Newly adherent QN cells are immature nestin$^+$ proliferating precursors

After sorting, QN cells were >98% pure, as revealed by their lack of surface epitopes used for sorting (Fig. 2*A*). These cells were also plated on glass coverslips for further immunocytochemical analysis. Many of the newly adherent QN cells rapidly flattened out and exhibited relatively phase-dark and epithelioid morphology (Fig. 2*C*). Most of these cells (~65–75%) were BrdU$^+$, after a single BrdU injection given *in vivo* 2 hr before killing (Fig. 2*B,D*), thus identifying them as actively proliferating. Almost all of the QN cells (~90–95%) were nestin-immunoreactive (Fig. 2*B,D*), which is characteristic of immature neuroepithelial cells (Maric et al., 2000c). Few of these cells (<5%) expressed either neuron-specific surface (ChTx and TnTx) or cytoplasmic (TuJ1) epitopes, and none exhibited epitopes characteristic of astroglial (GFAP), oligodendroglial (O4), or microglial (OX42) phenotypes (Fig. 2*B*). In addition, <2% of sorted QN cells stained with Annexin V (Fig. 2, legend) or propidium iodide (data not shown). Thus, at the time of their initial adherence, many QN cells were actively proliferating, and almost all were devoid of epitopes indicative of differentiation.

Neuronal, neuroglial, and oligoglial cells are immature nestin$^+$ progenitors

After sorting by positive selection, putative neuronal progenitors (NPs), neuroglial progenitors (NGPs), and oligoglial progenitors (OGPs) were immunolabeled with anti-nestin antibody, and the number of nestin$^+$ cells in each population was reanalyzed by flow cytometry. The results from three independent experiments revealed that immature nestin$^+$ cells predominated in each subpopulation, with most of these cells (94 ± 1.3%, mean ± SEM) composing the NGP population, followed by 83 ± 5% composing the NP population and 70 ± 4% composing the OGP population. The culturing of these cells under different growth conditions further revealed that significant fractions of each progenitor population exhibited the ability to expand and to generate variably restricted progeny of neuronal and glial phenotypes (Tables 2–4). These findings indicated that the sorted progenitor populations were predominantly in an immature state but were more restricted in generating multipotent neuronal and glial lineages compared with QN neural precursor cells (Tables 1–4).

Differential distributions of bFGF, FGFR-1, EGF, and EGFR

Approximately 80% of QN precursors expressed FGFR-1, and approximately one-third exhibited immunodetectable bFGF (Fig. 3*A1,A2,B1*). In contrast, relatively few of these cells were either EGF$^+$ (<5%) or EGFR$^+$ (~12%) (Fig. 3*A3,A4,B1*). Comparable proportions of neuronal and neuroglial progenitors expressed immunodetectable bFGF and FGFR-1, whereas EGF was only detectable in ~8% of neuronal progenitors and in <5% of neuroglial progenitors (Fig. 3*B2,B3*). EGFR immunoreactivity was more widely expressed among neuronal than neuroglial progenitors, although the number of EGFR$^+$ cells in the former population did not exceed 40% (Fig. 3*B2,B3*). Few oligoglial progenitors (<5%) were immunopositive for bFGF, EGF, or EGFR,

whereas only ~30% of these cells were FGFR-1$^+$ (Fig. 3*B4*). Thus, FGFR-1 was more widely expressed than bFGF among neural precursors and progenitors, and both were generally more abundant than either EGF or EGFR in each of the subpopulations.

Effects of bFGF and EGF on self-renewal and differentiation of QN cells

The highly contrasting expressions of bFGF and EGF and their corresponding receptors by neural precursors led us to investigate their possible roles in the regulation of proliferative and differentiating potentials of these cells. Sorted QN cells were plated at clonal density and cultured in Neurobasal and B27 medium containing bFGF, EGF, or both for 1 week. This allowed us to characterize the resulting phenotypes derived from individual cells. Inclusion of 10 ng/ml bFGF in the culture medium most often resulted in clonal expansion of QN neural precursors into epithelial-like monolayers, each composed of ~60–70 contiguous cells (Fig. 4). In fact, ~73% of the isolated neural precursors had expanded into epithelial monolayers composed only of immature cells, which were phenotypically identical to the original nestin$^+$BrdU$^{+/-}$ QN founder cells (Fig. 4*C*, Table 1) and did not express either intracellular or surface epitopes characteristic of differentiating neurons or glia. Approximately six symmetrical cell divisions (without cell death) would generate monolayers composed of ~60–70 cells over 7 d in culture. Only a few (~5%) QN precursors generated progeny that differentiated (Table 1). The remaining QN cells remained solitary and did not proliferate. Solitary cells that survived, which could be phenotyped, were either immature precursors or differentiating neurons or glia (Table 1). The presence of rare differentiating phenotypes may reflect a low probability that either QN precursors can differentiate in this medium or few newly committed progenitors, which do not yet express surface epitopes, were included in the QN population after sorting.

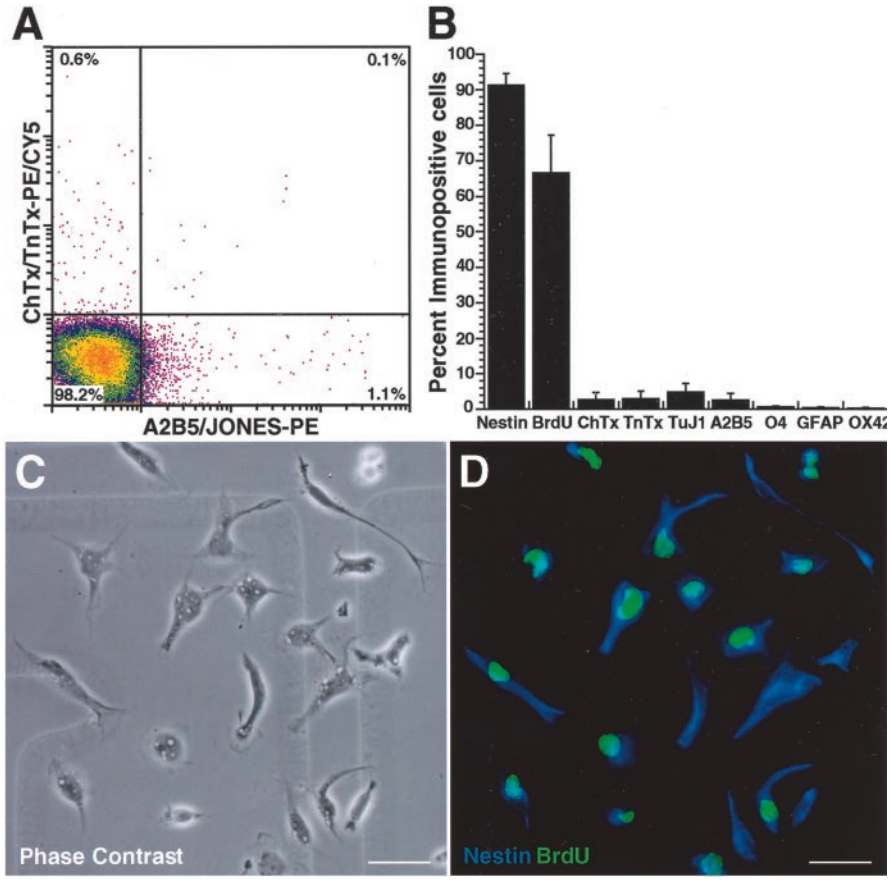

Figure 2. Quintuple epitope-negative cells are immature proliferating precursors. QN cells were sorted using the negative selection FACS strategy outlined in Figure 1. *A*, An aliquot of the sorted QN cells was reanalyzed, using the same electronic gates used for sorting. The *pseudocolor dot density plot* shows that the sorted cells consist primarily of neural precursors, which account for >98% of the population, with <2% of the cells expressing ChTx, TnTx, A2B5, or JONES. The percentage of Annexin V$^+$ cells in the QN population after sorting averaged 1.5 ± 0.2% (mean ± SEM; $n = 29$). *B–D*, Sorted QN cells, which had been pulse-labeled *in vivo* with BrdU for 2 hr (see Materials and Methods), were allowed to adhere on glass coverslips for 1 hr and then processed for BrdU incorporation and expression of epitopes characteristic of immature precursors (nestin) or differentiating neurons (ChTx, TnTx, and TuJ1), astrocytes (GFAP), neuroglial progenitors (A2B5), oligodendrocytes (O4), and microglia (OX42). *C*, Phase contrast microscopy illustrates a wide range of cell morphologies, including cell body elongations and process formation, which are indicative of the spontaneous motility exhibited by many of these cells. *D*, All of the cells in the field are nestin$^+$ (*blue* fluorescence), and most are BrdU$^+$ (*green* fluorescence) and therefore actively proliferating. The *bar graph* in *B* summarizes the distribution of epitopes detected among newly adherent precursors and represents the percentage (mean ± SEM) of immunopositive cells from three or more independent determinations. Rare cells (<5%) exhibit intracellular differentiating epitopes, and <2% exhibit surface differentiating epitopes. Scale bars, 20 μm.

Inclusion of 10 ng/ml EGF in the medium led to much less expansion of QN precursors, with many cells (26%) becoming pyknotic over the 7 d culture (Table 1). Solitary survivors were equally divided between immature precursors and committed neuronal or glial phenotypes (Table 1). Inclusion of both bFGF and EGF primarily generated either clusters of proliferating precursors (Fig. 4, Table 1) or clusters of cells that included a mixture of proliferating precursors and those differentiating into neuronal, oligodendroglial, and astrocyte type 1 progenitors (Fig. 5, Table 1). These multipotential clusters of differentiating phenotypes were typically composed of ~70–90 cells, ~50% of which exhibited either neuronal or astroglial epitopes. Comparative analysis showed that inclusion of EGF with bFGF increased the proportion of multipotential clusters by 10-fold relative to those expanding in medium with bFGF alone (see Table 1). Almost all of the differentiating progeny of QN cells were nestin$^+$, and approximately one-third were BrdU$^+$. Neuronal progenitors often appeared randomly scattered among the proliferating neural precursor progeny, whereas proliferating radial forms of astrocytes were often arrayed adjacent to proliferating and postmitotic astroglial cells with epithelioid morphologies. In some fields, nestin$^+$GFAP$^-$ bipolar cells with elongated morphologies were found transforming into epithelioid shapes, which were nestin$^+$GFAP$^+$. GFAP$^-$ bipolar cells were typically vimentin$^+$ (data not shown) and, therefore, most likely radial glial cells in an earlier stage of the astrocyte lineage. Rare clones (~1%) were composed of either type 2 astrocytes or oligodendrocytes (Table 1). Approximately one-fourth of the cells remained solitary and when phenotyped were either immature and undifferentiated or differentiated into neuronal or mostly radial glial phenotypes (Table 1). These qualitative comparisons of clones derived from isolated QN precursors demonstrate that (1) initial cell–cell con-

Table 1. Clonal analyses of bFGF and EGF effects on sort-purified neural precursors

Cell phenotype	bFGF	EGF	bFGF + EGF
Expanded cells			
Self-renewing	72 (73)	9 (12)	72 (33)
Multipotential	3 (3)	5 (7)	70 (32)
Bipotential	1 (1)	0 (0)	7 (3)
Neuronal	0 (0)	0 (0)	5 (2)
Astroglial (type 1)	1 (1)	6 (8)	8 (4)
Astroglial (type 2)	0 (0)	0 (0)	3 (1)
Oligodendroglial	0 (0)	0 (0)	1 (1)
Nonexpanded cells			
Pyknotic	12 (12)	19 (26)	14 (6)
Precursor	5 (5)	16 (22)	9 (4)
Neuronal	2 (2)	3 (4)	3 (1)
Radial glia	1 (1)	4 (5)	21 (10)
Astroglial (type 1)	2 (2)	8 (11)	2 (1)
Astroglial (type 2)	0 (0)	2 (3)	1 (1)
Oligodendroglial	0 (0)	1 (2)	2 (1)
Total clones studied	99	73	218

The effects of bFGF and EGF on clonal expansion and differentiation of neural precursors are shown. Neural precursors were sorted as outlined in Figure 1 and plated at clonal density in medium containing 10 ng/ml bFGF, 10 ng/ml EGF, or both, and the numbers of cells that either expanded (generating two or more progeny) or remained solitary (nonexpanded) after 7 d in culture were quantified, and their immunophenotype was characterized. The progeny of expanded clones were classified into the following categories according to their patterns of epitope expression: (1) self-renewing, consisting of only undifferentiated nestin$^+$ neural precursors, which lacked any of the differentiating epitopes, as exemplified by those in Figure 4; (2) multipotential, consisting of cells progressing along neuronal, astroglial, neuroglial, or oligodendroglial lineages, typical of those in Figure 5; (3) bipotential, consisting of cells progressing along neuroglial or oligodendroglial lineages; (4) neuronal, which included cells exhibiting either TuJ1$^+$A2B5$^-$TnTx$^+$, TuJ1$^+$A2B5$^+$TnTx$^-$ or TuJ1$^+$A2B5$^+$TnTx$^+$ phenotypes; (5) astroglial (type 1), consisting only of cells immunoidentified as A2B5$^-$GFAP$^+$; (6) astroglial (type 2), consisting only of cells immunoidentified as A2B5$^+$GFAP$^+$; and (7) oligodendroglial, consisting only of cells immunoidentified as A2B5$^+$O4$^+$, A2B5$^-$O4$^+$, or both. Solitary cells, which did not expand over 7 d in culture, were characterized as pyknotic and nonviable (identified either morphologically or using propidium iodide staining) or as belonging to one of six immunoidentified phenotypes: (1) immature nestin$^+$ precursors; (2) neuronal; (3) radial glia, which exhibited elongated bipolar morphologies and were vimentin$^+$ or nestin$^+$ but TuJ1$^-$GFAP$^-$A2B5$^-$TnTx$^-$; (4) astroglial (type 1); (5) astroglial (type 2); and (6) oligodendroglial. Data depict the number of founder clones studied in the three growth conditions. The numbers in parentheses are the relative percentages of the founder cells, which either expanded and generated self-renewing or differentiating progeny or did not expand but died or differentiated. The results in this and subsequent tables are derived from at least three independent experiments. Inclusion of bFGF in defined medium sustains proliferation but little differentiation of neural precursor cells. EGF in defined medium without bFGF supports little proliferation or differentiation. bFGF and EGF together in defined medium promote proliferation of neural precursors and differentiation of multiple phenotypes.

Table 2. Clonal analyses of bFGF and EGF effects on sort-purified neuronal progenitors

Cell phenotype	bFGF	EGF	bFGF + EGF
Expanded cells			
Self-renewing	3 (5)	1 (2)	4 (3)
Multipotential	2 (4)	2 (4)	6 (4)
Bipotential	0 (0)	0 (0)	2 (1)
Neuronal	12 (21)	3 (6)	35 (24)
Astroglial (type 1)	2 (4)	4 (8)	5 (4)
Astroglial (type 2)	0 (0)	0 (0)	0 (0)
Oligodendroglial	0 (0)	1 (2)	1 (1)
Nonexpanded cells			
Pyknotic	6 (11)	10 (19)	17 (12)
Precursor	3 (5)	0 (0)	2 (1)
Neuronal	24 (43)	27 (53)	65 (44)
Radial glia	1 (2)	1 (2)	1 (1)
Astroglial (type 1)	3 (5)	2 (4)	6 (4)
Astroglial (type 2)	0 (0)	0 (0)	0 (0)
Oligodendroglial	0 (0)	0 (0)	1 (1)
Total clones studied	56	51	145

The effects of bFGF and EGF on clonal expansion and differentiation of neuronal progenitors are shown. Neuronal progenitors were sorted as outlined in Figure 1 and then cultured and quantified using the strategy outlined in the legend of Table 1. The data show that bFGF, with or without EGF, primarily supports cells progressing along a neuronal lineage and neuronal differentiation with limited proliferation.

Table 3. Clonal analyses of bFGF and EGF effects on sort-purified neuroglial progenitors

Cell phenotype	bFGF	EGF	bFGF + EGF
Expanded cells			
Self-renewing	7 (7)	1 (1)	9 (5)
Multipotential	9 (8)	2 (2)	18 (11)
Bipotential	37 (35)	10 (11)	51 (30)
Neuronal	7 (7)	3 (3)	5 (3)
Astroglial (type 1)	0 (0)	1 (1)	3 (2)
Astroglial (type 2)	3 (2)	7 (8)	11 (7)
Oligodendroglial	6 (6)	2 (2)	14 (8)
Nonexpanded cells			
Pyknotic	5 (5)	29 (32)	6 (4)
Precursor	4 (4)	7 (8)	6 (4)
Neuronal	11 (10)	9 (10)	4 (2)
Radial glia	1 (1)	3 (3)	5 (3)
Astroglial (type 1)	2 (2)	3 (3)	3 (2)
Astroglial (type 2)	4 (4)	6 (7)	5 (3)
Oligodendroglial	10 (9)	8 (9)	27 (16)
Total clones studied	106	91	167

The effects of bFGF and EGF on clonal expansion and differentiation of neuroglial progenitors are shown. Neuroglial progenitors were sorted as outlined in Figure 1 and then cultured and quantified using the strategy outlined in the legend of Table 1. The data show that bFGF, with or without EGF, predominantly promotes neuronal and glial lineage progressions occurring from single founder cells.

Table 4. Clonal analyses of bFGF and EGF effects on sort-purified oligoglial progenitors

Cell phenotype	bFGF	EGF	bFGF + EGF
Expanded cells			
Self-renewing	1 (2)	0 (0)	3 (3)
Multipotential	3 (5)	2 (3)	3 (3)
Bipotential	6 (11)	4 (6)	8 (7)
Neuronal	4 (7)	3 (4)	3 (3)
Astroglial (type 1)	0 (0)	0 (0)	0 (0)
Astroglial (type 2)	2 (3)	2 (3)	5 (4)
Oligodendroglial	7 (12)	5 (7)	22 (19)
Nonexpanded cells			
Pyknotic	6 (11)	35 (50)	10 (9)
Precursor	2 (3)	3 (4)	5 (4)
Neuronal	3 (5)	2 (3)	3 (3)
Radial glia	0 (0)	0 (0)	1 (1)
Astroglial (type 1)	0 (0)	0 (0)	1 (1)
Astroglial (type 2)	2 (4)	5 (7)	4 (3)
Oligodendroglial	21 (37)	9 (13)	46 (40)
Total clones studied	57	70	114

The effects of bFGF and EGF on clonal expansion and differentiation of oligodendroglial progenitors are shown. Oligodendroglial progenitors were sorted as outlined in Figure 1 and then cultured and quantified using the strategy outlined in the legend of Table 1. The data show that bFGF, with or without EGF, primarily promotes oligodendroglial lineage progression and oligodendroglial differentiation.

tact is not required for either precursor cell expansion or progenitor cell proliferation and lineage progression; (2) bFGF sustains proliferation of precursors without significant differentiation, whereas EGF is relatively ineffective; and (3) bFGF and EGF together support both proliferation of neural precursors and their differentiation along neuronal and glial lineages.

In a separate series of experiments, QN cells were plated at clonal density and expanded for 7 d in bFGF-containing medium. The resulting progeny were then passaged and re-expanded in the medium with fresh bFGF, EGF, or both. The passaged progeny continued to proliferate in medium with fresh bFGF, remaining in an undifferentiated (nestin$^+$BrdU$^{+/-}$) neural precursor state (data not shown). However, inclusion of both EGF and bFGF in passaged cultures supported both continued proliferation of immature precursors and progression along neuronal and glial lineages (data not shown). Thus, both self-renewing and multipotential properties could be retained after passage, depending on the growth factor inclusions. These results further demonstrate that QN cells exhibit the defining characteristics of neural stem cells (i.e., proliferation and lineage progres-

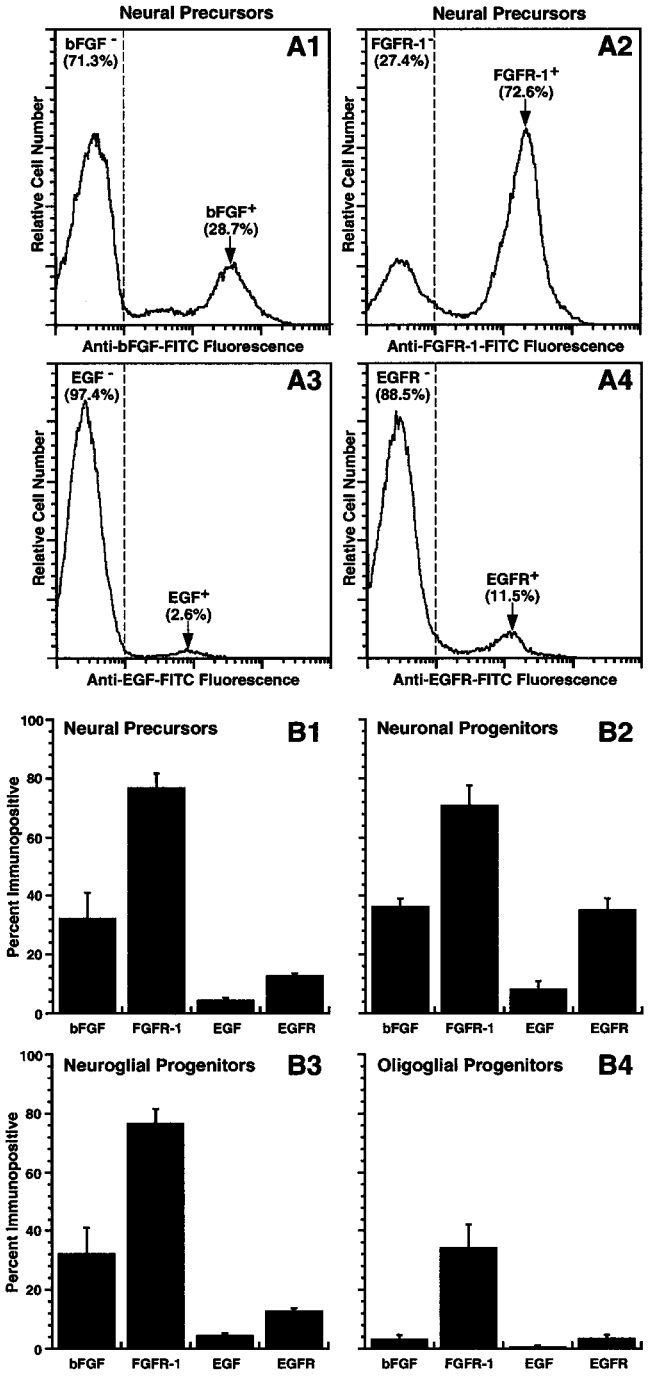

Figure 3. Differential distributions of bFGF, FGFR-1, EGF, and EGFR among neural precursors and progenitors. Neural precursors and neuronal, neuroglial, and oligoglial progenitors were isolated as described in Figure 1 and then profiled for bFGF, FGFR-1, EGF, or EGFR expression by flow cytometry. *A1–A4*, Frequency histograms of QN neural precursors immunostained for the growth factors and their corresponding receptors show that most cells express FGFR-1, and many exhibit bFGF, whereas few cells are either EGF $^{+}$ or EGFR $^{+}$. *B1–B4*, *Bar plots* summarizing the immunocytochemical results (means $\pm$ SEM) of three independent experiments reveal wider distributions of FGFR-1 and bFGF among sorted neural precursors and neuronal, neuroglial, and oligoglial progenitors compared with those obtained for EGF and EGFR.

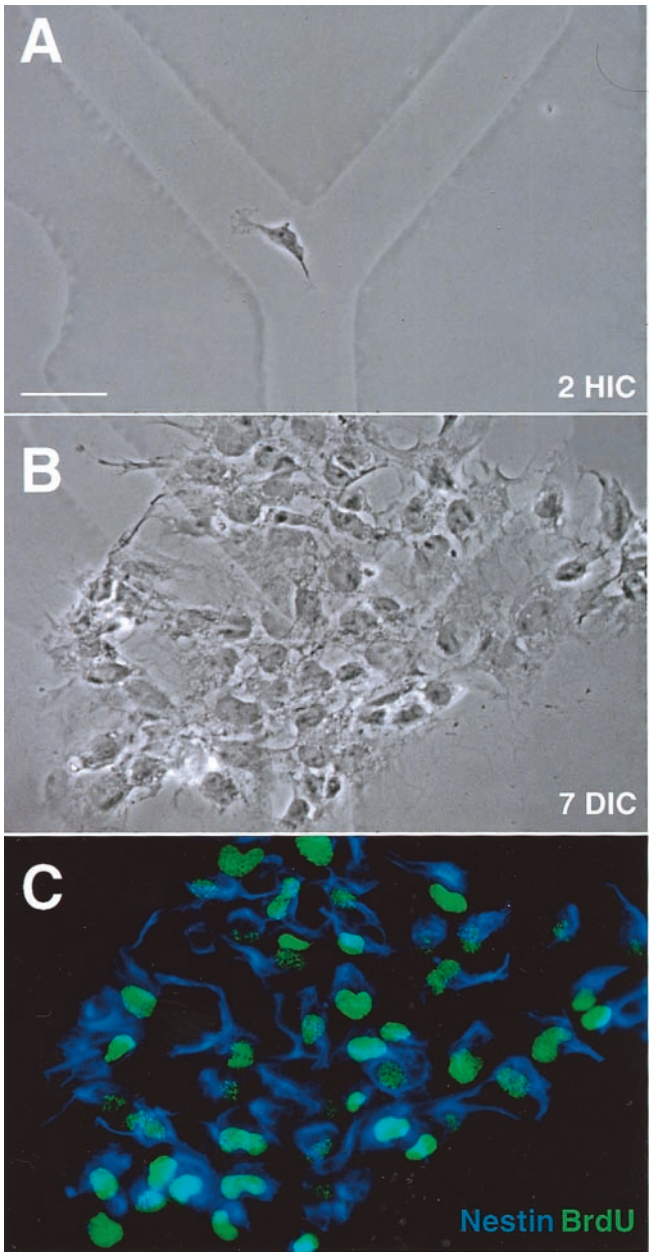

Figure 4. Typical clonal expansion of neural precursor cells in medium with bFGF. Neural precursors were sorted by negative selection as described in Figure 1 and then plated at clonal density in medium containing 10 ng/ml bFGF and maintained undisturbed for 1 week. *A*, A newly adherent neural precursor cell was photographed with phase contrast optics at 2 hr in culture (*HIC*) to reveal its location with respect to the underlying alphanumeric grid. *B*, The resulting progeny derived from this precursor formed an epithelial monolayer of morphologically similar cells after 7 d in culture (*DIC*), as is evident from the rephotographed field. In this representative example, the founder neural precursor cell generates 63 epithelial-like cells, 60 of which are viable and 3 of which are pyknotic. *C*, To characterize immature and differentiating neuronal and glial cell phenotypes in this and other experiments, a multiepitope staining protocol was used to reveal the expression of specific surface (ChTx, TnTx, A2B5, and O4), cytoplasmic (nestin, TuJ1, and GFAP), and nuclear (BrdU) epitopes. The cells were cumulatively labeled with BrdU for 24 hr before termination of culture and immunocytochemical processing. Nestin immunoreactions are shown in *blue*, whereas BrdU incorporation into DNA in the nucleus is shown in *green*. In this representative example, the viable neural precursor-derived progeny consist of 44 nestin $^{+}$BrdU $^{+}$ and 16 nestin $^{+}$BrdU $^{-}$ cells. No other differentiating epitopes are expressed by these cells (data not shown), indicating that the founder precursor cell self-renewed without differentiating. Scale bar, 20 μm.

sion among cells plated at clonal density and self-renewal and differentiation after passage).

Although we did not perform a complete dose–response study of bFGF and EGF effects on the proliferative and differentiating potential of neural stem cells, we did try a 10-fold larger dose (100

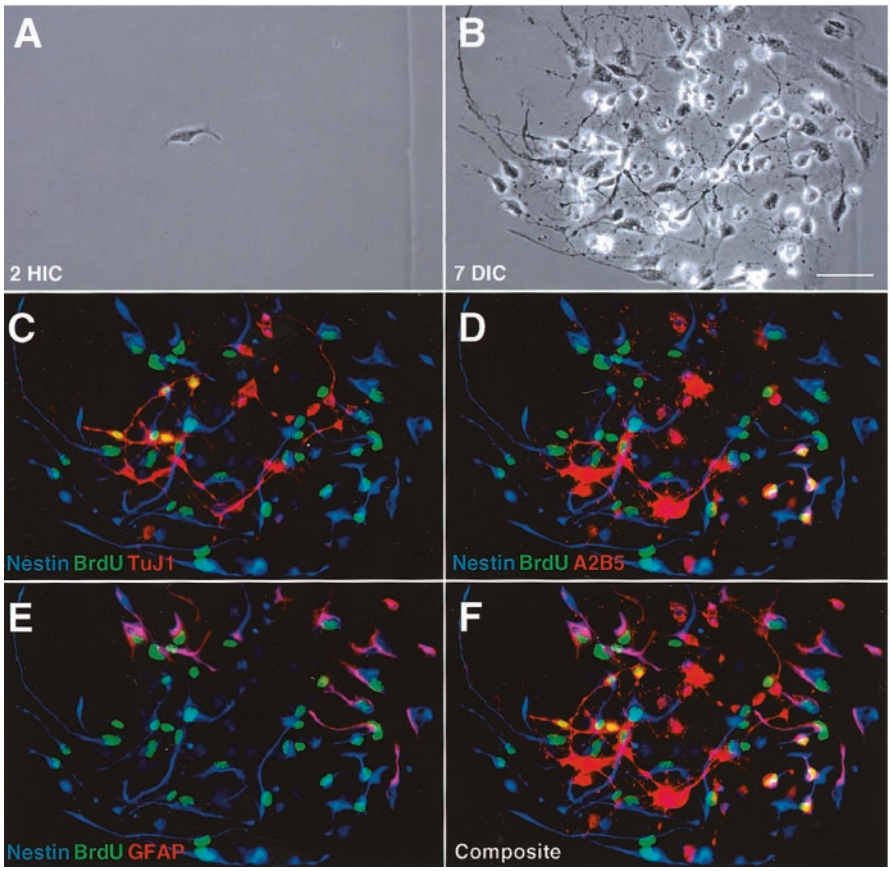

Figure 5. Typical clonal expansion of neural precursor cells in medium with bFGF and EGF. Neural precursors were cultured at clonal density in the presence of 10 ng/ml bFGF and 10 ng/ml EGF, maintained undisturbed for 1 week, and then labeled with BrdU and immunophenotyped for differentiating epitopes. In this representative example, a founder neural precursor cell (*A*) generates a complex array of phase-dark and phase-bright progeny (*B*) totaling 87 cells, 72 of which are viable and 15 of which are pyknotic. *C–F*, Immunostaining reveals variable numbers of progeny expressing differentiating epitopes characteristic of neuronal, astroglial, and oligodendroglial cell lineages, which have been visualized using different fluorochrome-conjugated immunoreagents identified in each *panel*. Multiepitope staining shows that the progeny can be phenotyped as follows: seven nestin $^+$BrdU $^-$ and six nestin $^+$BrdU $^+$ precursors; one nestin $^+$BrdU $^-$ cell and seven nestin $^+$BrdU $^+$ cells with radial glial morphologies; five nestin $^+$BrdU $^+$TuJ1 $^+$ and three nestin $^+$BrdU $^-$TuJ1 $^+$ neuronal progenitors; four nestin $^-$BrdU $^-$TuJ1 $^+$ neurons; four nestin $^+$BrdU $^+$A2B5 $^+$ and nine nestin $^+$BrdU $^-$A2B5 $^+$ neuroglial or oligodendroglial progenitors; 10 nestin $^+$BrdU $^-$A2B5 $^+$TuJ1 $^+$ neuronal progenitors; and three nestin $^+$BrdU $^+$GFAP $^+$ astroglial type 1 progenitors and three nestin $^+$BrdU $^-$GFAP $^+$ differentiating astrocyte type 1 progenitors. *2 HIC*, 2 hr in culture; *7 DIC*, 7 d in culture. Scale bar, 20 μm.

ng/ml) of each growth factor in the Neurobasal and B27 medium and cultured the cells undisturbed for 7 d. In addition, we separately cultured neural stem cells in media that were replenished with fresh 10 ng/ml bFGF, 10 ng/ml EGF, or both every 48 hr during the 7 d period of clonal expansion. In either case, we found no significant difference in the phenotypic outcomes compared with those described above. Thus, the marked difference in self-renewal of neural stem cells in the presence of bFGF compared with EGF may well reflect the fact that few of these cells (~11%) actually express the EGF receptor, whereas most (~75%) exhibit the receptor for bFGF (Fig. 3).

In some experiments, we also tested the effects of bFGF withdrawal on clonal expansion of neural stem cells over 7 d in culture. Withdrawal of bFGF within 24 hr of plating prevented self-renewal of neural stem cells and induced differentiation, predominantly along the astrocyte type 1 lineage. In contrast, withdrawal of bFGF after 5 d in culture did not overtly affect proliferation of the self-renewing neural stem cell progeny when examined 2 d later but did produce a significant increase in the number of neuronal and astroglial progeny. The limited effect of bFGF withdrawal at 5 d on self-renewal of neural stem cell progeny may reflect the possible contribution of endogenous bFGF expressed in 64% of these cells at this stage in culture (data not shown), which represents a twofold increase compared with that observed at the time of plating (Fig. 3).

Differential effects of bFGF and EGF on NP, NGP, and OGP expansion

Putative NPs plated at clonal density and cultured for 7 d in medium containing bFGF, EGF, or both either remained solitary or generated progeny, which primarily progressed along a neuronal lineage (Table 2). Most of the progeny of expanded NP clones clustered in groups of up to 20 cells. Thus, this outcome was likely to be derived from approximately four or five cell divisions. Immunophenotyping revealed that all progeny were TuJ1 $^+$, with many also expressing nestin, indicative of an immature neuronal state. In general, <10% of these cells were BrdU $^+$ after a cumulative 24 hr exposure with BrdU at the end of the 1 week period. Many of the newly postmitotic neurons extended processes several cell body diameters in length. These cells exhibited the same surface epitopes (ChTx $^+$TnTx $^+$) used for positive selection. ChTx and TnTx signals were extensively colocalized in the majority of the neuronal progeny.

Inclusion of bFGF with or without EGF sustained the same relative percentage (~21–24%) of NP cells undergoing neuronal lineage progression (Table 2). Only 6% of the cells plated in medium containing EGF generated progeny progressing along a neuronal lineage. However, EGF was as effective as bFGF in supporting the survival and differentiation of solitary progenitors into neurons (Table 2). Although neuronal lineage progression and differentiation predominated in the presence of bFGF, other phenotypes also occurred at lower frequencies. Small fractions of cells (~3–5%) expanded, either generating immature precursors or forming clusters of neuronal, astroglial, and oligodendroglial phenotypes (multipotential) or generating type 1 astrocytes. In medium with EGF alone, there were approximately as many cells progressing along an astroglial (type 1) lineage as those that expanded and differentiated into neurons. These latter results indicate that the positively selected subpopulation with surface epitopes characteristic of neuronal progenitors is not entirely restricted to a neuronal lineage.

Putative NGPs primarily formed clusters of ~20–25 cells, which were either A2B5 $^+$TuJ1 $^+$ or A2B5 $^+$TuJ1 $^-$ (Table 3). Most of the progeny from expanded NGP clones were nestin $^+$, and many were BrdU $^+$, indicating that these cells were immature and actively proliferating. Clonal analyses revealed that clusters with neuronal and putative glial phenotypes predominated (30–35%) when bFGF was included in the culture medium, with or without EGF (Table 3). In medium with EGF only 11% of the progeny exhibited this duality of phenotypes. Smaller fractions of

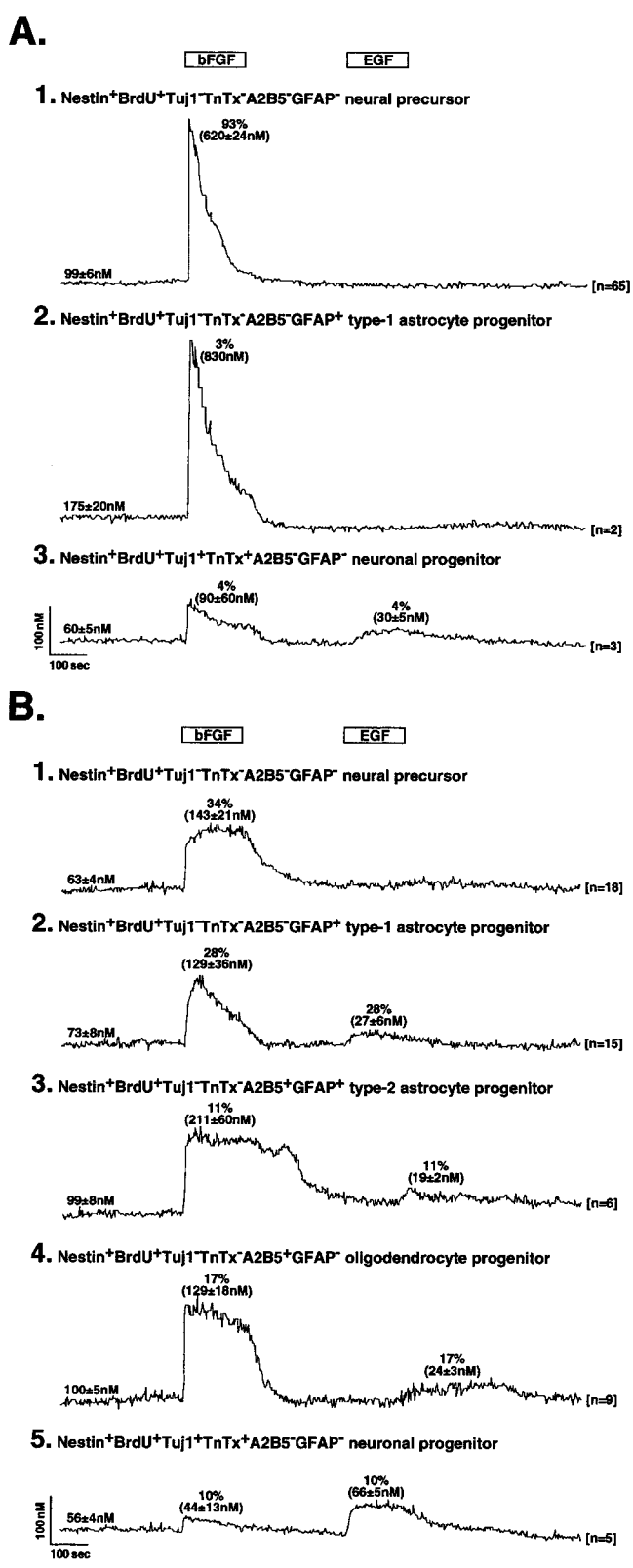

Figure 6. Calcium imaging of bFGF and EGF effects on neural precursor cell progeny. *A*, Neural precursors were cultured in medium with 10 ng/ml bFGF for 7 d and then imaged for Ca^{2+} responses to bFGF and EGF. After imaging, the cells were phenotyped for their expression of immature and differentiating epitopes. *A1*, Immunophenotyping reveals that 93% of the QN cell progeny are self-renewing precursor cells, all of which respond to bFGF with a rapidly rising, primarily transient Ca^{2+}_c signal with an average peak amplitude at 620 ± 24 nM (mean ± SEM), but none respond to EGF. *A2*, Rare cells identified as astrocyte type 1 progenitors (~3% of total progeny) exhibit similar responses to bFGF, with the peak response averaging ~830 nM, but do not respond to EGF. This contrasts with the responses of astrocyte type 1 progenitors cultured in medium containing bFGF and EGF (see *B2*). *A3*, Few cells identified as neuronal progenitors (~4% of total progeny) respond to both bFGF and EGF, with the average response peaking at 90 ± 60 and 30 ± 5 nM, respectively. *B*, Calcium imaging and immunophenotyping were also performed on QN cells cultured for 7 d in medium containing 10 ng/ml bFGF and 10 ng/ml EGF. *B1*, In contrast to bFGF-expanded QN cell progeny, self-renewing precursors account for only ~34% of the total cells in bFGF and EGF cultures. All of these precursors respond to bFGF with a rapidly rising sustained Ca^{2+}_c signal, with an average amplitude of 143 ± 21 nM, but none respond to EGF, similar to results on those self-renewing in medium with bFGF. *B2*, Cells identified as type 1 astrocyte progenitors in these cultures exhibited rapidly rising transient Ca^{2+}_c responses to bFGF (average amplitude, 129 ± 36 nM) and low-amplitude responses to EGF (27 ± 6 nM). *B3*, Type 2 astrocyte progenitors express rapidly rising and sustained Ca^{2+}_c responses to bFGF (211 ± 60 nM) and low-amplitude responses to EGF (19 ± 2 nM). *B4*, Oligodendrocyte progenitors respond to bFGF (129 ± 18 nM) with rapidly rising and sustained Ca^{2+}_c responses and to EGF with low-amplitude signals (24 ± 3 nM). *B5*, Neuronal progenitors exhibit rapidly rising and relatively sustained low-amplitude Ca^{2+}_c responses to both bFGF (44 ± 13 nM) and EGF (66 ± 5 nM). The cells were continuously superfused with NPM at 37°C before and during pharmacological manipulation. *Open horizontal bars* depict the duration of exposure to bFGF or EGF. The *numbers* at the *beginning* of each *trace* represent the average Ca^{2+}_c baseline (mean ± SEM) for each cell phenotype recorded. The *numbers* at the *end* of each *trace* represent the sample size (i.e., the number of cells recorded for each phenotype). The *numbers* in *parentheses* depict the peak Ca^{2+}_c levels (mean ± SEM) after response to bFGF or EGF. The *values above* the *peak calcium levels* depict the percentages of total QN cell progeny with a designated phenotype, which resulted after culture in bFGF- or bFGF- and EGF-containing media.

progeny (≤10%) evolved along each of the other characterized phenotypes. In contrast to the lineages derived from QN and NP cells, a detectable number of progeny derived from isolated NGP clones also differentiated into oligodendroglia or astroglia (type 2) instead of astroglia (type 1). Oligodendroglia accounted for the greatest number of solitary survivors when both bFGF and EGF were included (Table 3). These results are consistent with the premise that the sorted NGP subpopulation consisted primarily of bipotential progenitors.

Putative OGPs either progressed along the oligodendroglial lineage or differentiated into oligodendroglia (Table 4). Lineage progression from expanded OGP clones was most evident in medium containing both bFGF and EGF, with ~20–25 cells constituting a typical cluster. The natural progression from nestin$^+$BrdU$^+$A2B5$^+$ immature progenitors to nestin$^+$A2B5$^+$O4$^+$ oligodendroglial progenitors to nestin$^-$A2B5$^-$O4$^+$ transitional oligodendrocytes was spatially arrayed in many of the fields surveyed. Oligodendroglial lineage progression and differentiation of progenitors into oligodendrocytes predominated, especially when bFGF was included, whereas other phenotypes occurred at much lower frequencies (Table 4). Cells progressing exclusively along the astroglial (type 1) lineage were typically absent.

bFGF- and EGF-induced calcium signaling

QN cells were cultured in medium with bFGF to promote self-renewal (Fig. 4) or in medium with bFGF and EGF to promote differentiation (Fig. 5). The cells were imaged after 7 d in culture, and their resting and evoked Ca^{2+}_c levels were recorded before and after stimulation with exogenous bFGF and EGF. The results revealed that virtually all of the self-renewing progeny of neural stem cells responded to bFGF by elevating their Ca_c^{2+} levels (Fig. 6*A1*). Rare astrocyte type 1 progenitor cells differentiating in the medium with bFGF exhibited Ca_c^{2+} responses generally similar to those recorded on neural precursors (Fig. 6*A2*), whereas rare neuronal progenitors differentiating in the same medium responded to both bFGF and EGF (Fig. 6*A3*). Similar to QN cell progeny expanding in bFGF, neural precursors expanding in

bFGF- and EGF-conditioned media produced Ca^{2+}_c responses to bFGF but not EGF (Fig. 6*B1*). However, virtually all of the neuronal and glial progeny of neural stem cells differentiating in the medium with bFGF and EGF responded to both growth factors (Fig. 6*B2–B5*). The bFGF-induced Ca^{2+}_c signals were rapidly rising and variable in amplitude and time course among precursors and progenitors. Most of the responses were relatively well sustained, and some briefly persisted after removal of bFGF (Fig. 6*B3*). bFGF-induced Ca^{2+}_c responses recorded on differentiating progenitors were consistently greater in peak amplitude than those evoked by EGF with the exception of those detected on neuronal progenitors, which were generally similar. The EGF-induced Ca^{2+}_c signals evoked in oligodendrocyte and type 2 astrocyte progenitors were noticeably delayed several minutes after exposure to EGF, whereas those elicited in type 1 astrocyte and neuronal progenitors were immediate. These results revealed that self-renewing neural precursors only responded to bFGF, whether they were exposed to EGF, whereas all of the progenitor phenotypes differentiating in bFGF and EGF responded to both growth factors.

Advantages of fluorescence-activated cell sorting

To ascertain the utility of using sort-purified neural precursor and progenitor cells to study differential effects of bFGF and EGF on self-renewal and differentiation, we also cultured unsorted neuroepithelial cells dissociated from E13 rat telencephalon (the heterogenic composition of which is depicted in Fig. 1) under the same growth conditions used for sorted cells. The cells in the unsorted cultures proliferated in the presence of bFGF but not EGF, similar to the results obtained with sorted neural precursor and progenitor cells. However, the composition of the expanded cell progeny was predominantly of differentiating neuronal and glial phenotypes, rather than self-renewing neural stem cells. This is in keeping with the fact that at this stage of development, both neural stem cells and progenitors predominantly express FGFR-1 (Fig. 3) and have the potential to proliferate in the presence of bFGF rather than EGF. However, because the starting population of viable neural stem cells before culture is only ~22% of the unsorted neuroepithelial cells (Fig. 1, second paragraph of Results), the proliferation in bFGF-containing medium is biased toward expanding neuronal and glial progenitors rather than neural stem cells. We have also observed that after 7 d in culture in the presence of bFGF, the expanding neuronal and glial progenitor populations of unsorted neuroepithelial cells totally predominate over the neural stem cell population, which at that point represents <5% of the total cells. These findings reinforced the importance and the utility of our sorting strategy to gain direct access to purified neural stem cells and different neural progenitor populations, which then allows for precise prospective studies of their biology, rather than using retrospective analyses, which are currently applied in numerous neural stem cell models involving heterogeneous neuroepithelial cells as the starting population.

Discussion

Salient findings

Surface ganglioside epitopes emerging among differentiating CNS cell phenotypes were exploited to isolate neural precursors and lineage-restricted progenitors directly from the E13 rat telencephalon using fluorescence-activated cell sorting. Neural precursors, which did not express differentiating or apoptotic epitopes, were sorted by negative selection. These cells expressed FGFR-1 and proliferated in defined medium containing bFGF, primarily self-renewing and generating more neural precursors. Inclusion of EGF with bFGF stimulated both self-renewal and multipotential differentiation of neural precursors, properties that were retained after passage, thus identifying these cells as neural stem cells. Neuronal and glial progenitors, sorted by positive selection, also expressed FGFR-1 but primarily differentiated into their respective phenotypes in media containing bFGF with or without EGF. Self-renewing progeny of neural stem cells expressed Ca^{2+}_c responses to bFGF, whereas differentiating progeny of these cells responded to both bFGF and EGF.

FACS isolation of neural stem and lineage-restricted progenitor cells

Most studies on neural stem cells have been performed retrospectively using heterogeneous populations of neuroepithelial cells, which have been selectively cultured in defined media with different growth factors. In these models, the phenotypic analysis of neuroepithelial cell-derived progeny was necessary to confirm the presence of cells with the self-renewing and multipotent characteristics of neural stem cells (Johe et al., 1996; Qian et al., 1998, 2000). Recently, neural stem cells have been sorted from fetal human brain tissue using surface epitopes and a positive selection strategy (Uchida et al., 2000). These cells both self-renewed and differentiated into neurons and astrocytes but not oligodendrocytes, indicating that cells with some of the properties of neural stem cells can be sorted from the embryonic CNS. Self-renewing neural stem cells with pluripotent capabilities have also been isolated from the adult murine ependymal and subventricular zones using surface epitope markers and flow cytometry (Rietze et al., 2001). In our study, we have developed a novel multiepitope surface-staining strategy in conjunction with fluorescence-activated cell sorting to directly isolate neural precursors by negative selection and progenitors by positive selection from the neuroepithelium of the embryonic rat telencephalon to study their lineage potentials *in vitro*. This newly devised positive and negative selection strategy targeted ganglioside and apoptotic epitopes, which are conserved not only among neuroepithelial cells from different CNS regions (Maric et al., 1999) but also from other species, including mouse and human (D. Maric and J. L. Barker, unpublished observations). Thus, this FACS strategy may be applied to sort putative neural stem and lineage-restricted progenitor cells from developing CNS tissues of different vertebrates for prospective cellular and molecular studies. Furthermore, the unique application of negative selection to isolate neural stem cells, as described here, may provide an additional advantage for these cells by eliminating any concerns about possible effects of labeling reactions used in positive selection on the biology of these cells. Naturally, further studies will be necessary to ascertain whether the results described here for the neuroepithelial model of E13 rat telencephalon can be generalized to other ages, species, and CNS regions.

Differential effects of bFGF and EGF on self-renewal and differentiation

Specific growth factors, including bFGF and EGF, emerge during CNS development *in vivo* and have often been used to study proliferation and differentiation of neuroepithelial cells *in vitro* (Gensburger et al., 1987; Murphy et al., 1990; Vescovi et al., 1993; Ghosh and Greenberg, 1995; Reynolds and Weiss, 1996; Qian et al., 1997; Ciccolini and Svendsen, 1998; Tropepe et al., 1999). The relative utility of these growth factors in self-renewal and differentiation of neuroepithelial cells has varied, presumably because of the heterogeneity inherent in the neuroepithelial cell popula-

tions that were investigated. In our study, direct isolation of more homogenous neural stem cells revealed that most expressed FGFR-1, whereas only a fraction were $EGFR^+$ and thus had the potential to respond to bFGF rather than EGF. Although many neural stem cells also exhibited immunoreactivity for bFGF, few cells initially plated at clonal density proliferated or survived in the absence of exogenous bFGF. However, when plated at high density in a medium without exogenous bFGF, many of these cells survived and proliferated, whereas some also differentiated. Withdrawal of exogenous bFGF at that point, when most of the expanded neural stem cell progeny exhibited immunoreactivity for bFGF and FGFR1, did not overtly affect proliferation of these cells but did promote limited differentiation. Although the cellular and molecular mechanisms underlying this switch in bFGF dependency have not been elucidated, it is possible that at some point, autocrine or paracrine bFGF and FGFR-1 signaling, or both, may play a increasing role in sustaining self-renewal and differentiation of neural stem cells *in vitro*.

Our results extend previous reports demonstrating growth factors and receptors in the early embryonic CNS (Wanaka et al., 1991; Kilpatrick and Bartlett, 1995; Ozawa et al., 1996; Kalyani et al., 1999) and are in keeping with those showing that EGFR expression becomes detectable later during neurogenesis (Threadgill et al., 1995; Kornblum et al., 1997). In this regard, previous studies have led to the consensus that bFGF is mitogenic at the beginning of neurogenesis. Exogenously applied bFGF, but not EGF, stimulated the initial proliferation of E13 rat cortical cells (Gensburger et al., 1987) and E10 mouse neuroepithelial cells (Kilpatrick and Bartlett, 1995). Neuroepithelial cells derived from E8.5 anterior neural plate tissue also proliferated in the presence of bFGF, but not EGF, whereas early embryonic dissociates of cortical and striatal germinal zones responded primarily to bFGF and secondarily to EGF (Tropepe et al., 1999). Furthermore, neuroepithelial cells derived from E10.5 rat neural tubes synthesized bFGF and FGFR-1 and responded to bFGF, but not EGF (Kalyani et al., 1999). Similar results were obtained with dissociates of E14 striatum, in which responsiveness to bFGF preceded the emergence of functional EGFR on cells expressing receptors to bFGF (Ciccolini and Svendsen, 1998). Together, these studies have suggested a model whereby bFGF-responsive precursors and progenitors divide symmetrically before EGF-responsive cells emerge, which expand through asymmetric divisions of bFGF-responsive cells (Santa-Olalla and Covarrubias, 1999; Martens et al., 2000). These findings are consistent with the results of our study, which showed that most neural stem cells isolated from E13 rat telencephalon were $FGFR\text{-}1^+$ (~80%), whereas few were $EGFR^+$ (~12%), and revealed that EGF receptor functions emerge as bFGF-responsive neural precursors transition into differentiating progenitor stages.

Ca^{2+} responses to both bFGF and EGF emerge with neural cell commitment

Differential effects of bFGF and EGF on expansion and differentiation of neural precursors and progenitors prompted us to investigate whether these growth factors play a role in $Ca^{2+}{}_c$ signaling and, if so, whether these effects were related to cell phenotype. Both growth factors have been shown to elevate $Ca^{2+}{}_c$ levels in a wide variety of cell phenotypes (Pandiella et al., 1988, 1989; Magni et al., 1991; Puro, 1991; Peppelenbosch et al., 1992; Peters et al., 1992; Merle et al., 1995; Munaron et al., 1995, 1997; Ma and Sansom, 2001), including neural crest cells (Distasi et al., 1995) and ganglionic neurons (Distasi et al., 1998). In addition, we have reported previously that bFGF-promoted proliferation of unsorted neuroepithelial cells isolated from the E13 rat telencephalon is Ca^{2+}-dependent, because expansion of these cells was markedly attenuated when extracellular Ca^{2+} and $Ca^{2+}{}_c$ were pharmacologically reduced (Ma et al., 2000). In the present study, we extend our findings by demonstrating that bFGF, but not EGF, evokes $Ca^{2+}{}_c$ responses in sort-purified, self-renewing neural stem cells, whereas both bFGF and EGF induce $Ca^{2+}{}_c$ signals in differentiating neuronal and glial progeny of these cells. Thus, the emergence of $Ca^{2+}{}_c$ responses to both growth factors correlated closely with neural stem cell commitment and lineage progression. Exactly how each growth factor receptor is coupled via signal transduction pathways to $Ca^{2+}{}_c$ regulation and how this signaling is related to self-renewal and lineage progression remain to be elucidated.

References

Anderson DJ (2001) Stem cells and pattern formation in the nervous system: the possible versus the actual. Neuron 30:19–35.

Baird A (1994) Potential mechanisms regulating the extracellular activities of basic fibroblast growth factor (FGF-2). Mol Reprod 39:43–48.

Cameron HA, McKay R (1998) Stem cells and neurogenesis in the adult brain. Curr Opin Neurobiol 8:677–680.

Chu VT, Gage FH (2001) Chipping away at stem cells. Proc Natl Acad Sci USA 98:7652–7653.

Ciccolini F, Svendsen CN (1998) Fibroblast growth factor 2 (FGF-2) promotes acquisition of epidermal growth factor (EGF) responsiveness in mouse striatal precursor cells: identification of neural precursors responding to both EGF and FGF-2. J Neurosci 18:7869–7880.

Distasi C, Munaron L, Laezza F, Lovisolo D (1995) Basic fibroblast growth factor opens calcium-permeable channels in quail mesencephalic neural crest neurons. Eur J Neurosci 7:516–520.

Distasi C, Torre M, Antoniotti S, Munaron L, Lovisolo D (1998) Neuronal survival and calcium influx induced by basic fibroblast growth factor in chick ciliary ganglion neurons. Eur J Neurosci 10:2276–2286.

Gage FH (2000) Mammalian neural stem cells. Science 287:1433–1438.

Gensburger C, Labourdette G, Sensenbrenner M (1987) Brain basic fibroblast growth factor stimulates the proliferation of rat neuronal precursor cells in vitro. FEBS Lett 217:1–5.

Ghosh A, Greenberg ME (1995) Distinct roles for bFGF and NT-3 in the regulation of cortical neurogenesis. Neuron 15:89–103.

Hebel R, Stromberg MW (1986) Anatomy and embryology of the laboratory rat. Worthsee, Germany: BioMed Verlag.

Hockfield S, McKay RD (1985) Identification of major cell classes in the developing mammalian nervous system. J Neurosci 5:3310–3328.

Johe KK, Hazel TG, Muller T, Dugich-Djordjevic MM, McKay RD (1996) Single factors direct the differentiation of stem cells from the fetal and adult central nervous system. Genes Dev 10:3129–3140.

Kalyani AJ, Mujtaba T, Rao MS (1999) Expression of EGF receptor and FGF receptor isoforms during neuroepithelial stem cell differentiation. J Neurobiol 38:207–224.

Kilpatrick TJ, Bartlett PF (1995) Cloned multipotential precursors from the mouse cerebrum require FGF-2, whereas glial restricted precursors are stimulated with either FGF-2 or EGF. J Neurosci 15:3653–3661.

Koopman G, Reutelingsperger CP, Kuijten GA, Keehnen RM, Pals ST, van Oers MH (1994) Annexin V for flow cytometric detection of phosphatidylserine expression on B cells undergoing apoptosis. Blood 84:1415–1420.

Kornblum HI, Geschwind DH (2001) Molecular markers in CNS stem cell research: hitting a moving target. Nat Rev Neurosci 2:843–846.

Kornblum HI, Hussain RJ, Bronstein JM, Gall CM, Lee DC, Seroogy KB (1997) Prenatal ontogeny of the epidermal growth factor receptor and its ligand, transforming growth factor alpha, in the rat brain. J Comp Neurol 380:243–261.

Ma R, Sansom SC (2001) Epidermal growth factor activates store-operated calcium channels in human glomerular mesangial cells. J Am Soc Nephrol 12:47–53.

Ma W, Maric D, Li B-S, Hu Q, Andreadis JD, Grant GM, Liu Q-Y, Shaffer KM, Chang Y-H, Zhang L, Pancrazio JJ, Pant HC, Stenger DA, Barker JL (2000) Acetylcholine stimulates cortical precursor cell proliferation *in*

vitro via muscarinic receptor activation and map kinase phosphorylation. Eur J Neursci 12:1–4.

Magni M, Meldolesi J, Pandiella A (1991) Ionic events induced by epidermal growth factor: evidence that hyperpolarization and stimulated cation influx play a role in the stimulation of cell growth. J Biol Chem 266:6329–6335.

Maric D, Maric I, Ma W, Lahojuji F, Somogyi R, Wen X, Sieghart W, Fritschy JM, Barker JL (1997) Anatomical gradients in proliferation and differentiation of embryoni. c rat CNS accessed by buoyant density fractionation: alpha 3, beta 3 and gamma 2 $GABA_A$ receptor subunit coexpression by post-mitotic neocortical neurons correlates directly with cell buoyancy. Eur J Neurosci 9:507–522.

Maric D, Maric I, Barker JL (1998) Buoyant density gradient fractionation and flow cytometric analysis of embryonic rat cortical neurons and progenitor cells. Methods 16:247–259.

Maric D, Maric I, Barker JL (1999) Flow cytometric strategies to study CNS development. In: Neuromethods, Vol 33 (Boulton AA, Baker GB, eds), pp 287–318. Totowa, NJ: Humana.

Maric D, Maric I, Barker JL (2000a) Developmental changes in cell calcium homeostasis during neurogenesis of the embryonic rat cerebral cortex. Cereb Cortex 10:561–573.

Maric D, Maric I, Barker JL (2000b) Dual video microscopic imaging of membrane potential and cytosolic calcium of immunoidentified embryonic rat cortical cells. Methods 21:335–347.

Maric D, Maric I, Chang Y-H, Barker JL (2000c) Stereotypic physiological properties emerge during early neuronal and glial lineage development in the embryonic rat neocortex. Cereb Cortex 10:729–747.

Martens DJ, Tropepe V, van Der Kooy D (2000) Separate proliferation kinetics of fibroblast growth factor-responsive and epidermal growth factor-responsive neural stem cells within the embryonic forebrain germinal zone. J Neurosci 20:1085–1095.

Martin SJ, Reutelingsperger CP, McGahon AJ, Rader JA, van Schie RC, LaFace DM, Green DR (1995) Early redistribution of plasma membrane phosphatidylserine is a general feature of apoptosis regardless of the initiating stimulus: inhibition by overexpression of Bcl-2 and Abl. J Exp Med 182:1545–1556.

Merle PL, Feige JJ, Verdetti J (1995) Basic fibroblast growth factor activates calcium channels in neonatal rat cardiomyocytes. J Biol Chem 270:17361–17367.

Morrison SJ, White PM, Zock C, Anderson DJ (1999) Prospective identification, isolation by flow cytometry, and in vivo self-renewal of multipotent mammalian neural crest stem cells. Cell 96:737–749.

Munaron L, Distasi C, Carabelli V, Baccino FM, Bonelli G, Lovisolo D (1995) Sustained calcium influx activated by basic fibroblast growth factor in Balb-c 3T3 fibroblasts. J Physiol (Lond) 484:557–566.

Munaron L, Antoniotti S, Distasi C, Lovisolo D (1997) Arachidonic acid mediates calcium influx induced by basic fibroblast growth factor in Balb-c 3T3 fibroblasts. Cell Calcium 22:179–188.

Murphy M, Drago J, Bartlett PF (1990) Fibroblast growth factor stimulates the proliferation and differentiation of neural precursor cells in vitro. J Neurosci Res 25:463–475.

Ozawa K, Uruno T, Miyakawa K, Seo M, Imamura T (1996) Expression of the fibroblast growth factor family and their receptor family genes during mouse brain development. Brain Res Mol Brain Res 41:279–288.

Pandiella A, Beguinot L, Velu TJ, Meldolesi J (1988) Transmembrane signalling at epidermal growth factor receptors overexpressed in NIH 3T3 cells: phosphoinositide hydrolysis, cytosolic Ca^{2+} increase and alkalinization correlate with epidermal-growth-factor-induced cell proliferation. Biochem J 254:223–228.

Pandiella A, Magni M, Lovisolo D, Meldolesi J (1989) The effect of epidermal growth factor on membrane potential: rapid hyperpolarization followed by persistent fluctuations. J Biol Chem 264:12914–12921.

Peppelenbosch MP, Tertoolen LG, den Hertog J, de Laat SW (1992) Epidermal growth factor activates calcium channels by phospholipase A2/5-lipoxygenase-mediated leukotriene C4 production. Cell 69:295–303.

Peters KG, Marie J, Wilson E, Ives HE, Escobedo J, Del Rosario M, Mirda D, Williams LT (1992) Point mutation of an FGF receptor abolishes phosphatidylinositol turnover and Ca^{2+} flux but not mitogenesis. Nature 358:678–681.

Puro DG (1991) A calcium-activated, calcium-permeable ion channel in human retinal glial cells: modulation by basic fibroblast growth factor. Brain Res 548:329–333.

Qian X, Davis AA, Goderie SK, Temple S (1997) FGF2 concentration regulates the generation of neurons and glia from multipotent cortical stem cells. Neuron 18:81–93.

Qian X, Goderie SK, Shen Q, Stern JH, Temple S (1998) Intrinsic programs of patterned cell lineages in isolated vertebrate CNS ventricular zone cells. Development 125:3143–3152.

Qian X, Shen Q, Goderie SK, He W, Capela A, Davis AA, Temple S (2000) Timing of CNS cell generation: a programmed sequence of neuron and glial cell production from isolated murine cortical stem cells. Neuron 28:69–80.

Rao MS (1999) Multipotent and restricted precursors in the central nervous system. Anat Rec 257:137–148.

Reynolds BA, Weiss S (1996) Clonal and population analyses demonstrate that an EGF-responsive mammalian embryonic CNS precursor is a stem cell. Dev Biol 175:1–13.

Rietze RL, Valcanis H, Brooker GF, Thomas T, Voss AK, Bartlett PF (2001) Purification of a pluripotent neural stem cell from the adult mouse brain. Nature 412:736–739.

Santa-Olalla J, Covarrubias L (1999) Basic fibroblast growth factor promotes epidermal growth factor responsiveness and survival of mesencephalic neural precursor cells. J Neurobiol 40:14–27.

Temple S (2001) The development of neural stem cells. Nature 414:112–117.

Threadgill DW, Dlugosz AA, Hansen LA, Tennenbaum T, Lichti U, Yee D, LaMantia C, Mourton T, Herrup K, Harris RC, Barnard JA, Yuspa SH, Coffey RJ, Magnuson T (1995) Targeted disruption of mouse EGF receptor: effect of genetic background on mutant phenotype. Science 269:230–234.

Tropepe V, Sibilia M, Ciruna BG, Rossant J, Wagner EF, van der Kooy D (1999) Distinct neural stem cells proliferate in response to EGF and FGF in the developing mouse telencephalon. Dev Biol 208:166–188.

Uchida N, Buck DW, He D, Reitsma MJ, Masek M, Phan TV, Tsukamoto AS, Gage FH, Weissman IL (2000) Direct isolation of human central nervous system stem cells. Proc Natl Acad Sci USA 97:14720–14725.

Vescovi AL, Reynolds BA, Fraser DD, Weiss S (1993) bFGF regulates the proliferative fate of unipotent (neuronal) and bipotent (neuronal/astroglial) EGF-generated CNS progenitor cells. Neuron 11:951–966.

Wanaka A, Milbrandt J, Johnson Jr EM (1991) Expression of FGF receptor gene in rat development. Development 111:455–468.

Weise B, Janet T, Grothe C (1993) Localization of bFGF and FGF-receptor in the developing nervous system of the embryonic and newborn rat. J Neurosci Res 34:442–453.